

# Holonomic quantum gates: A semiconductor-based implementation

Paolo Solinas,\* Paolo Zanardi,<sup>†</sup> Nino Zanghì,\* and Fausto Rossi<sup>†,‡</sup>

\* *Istituto Nazionale di Fisica Nucleare (INFN) and Dipartimento di Fisica,  
Università di Genova, Via Dodecaneso 33, 16146 Genova, Italy*

<sup>†</sup> *Institute for Scientific Interchange (ISI), Viale Settimio Severo 65, 10133 Torino, Italy*

<sup>‡</sup> *Istituto Nazionale per la Fisica della Materia (INFM) and Dipartimento di Fisica,  
Politecnico di Torino, Corso Duca degli Abruzzi 24, 10129 Torino, Italy*

We propose an implementation of holonomic (geometrical) quantum gates by means of semiconductor nanostructures. Our quantum hardware consists of semiconductor macroatoms driven by sequences of ultrafast laser pulses (*all optical control*). Our logical bits are Coulomb-correlated electron-hole pairs (excitons) in a four-level scheme selectively addressed by laser pulses with different polarization. A universal set of single and two-qubit gates is generated by adiabatic change of the Rabi frequencies of the lasers and by exploiting the dipole coupling between excitons

PACS numbers: Valid PACS appear here

## I. INTRODUCTION

In the recent years the interest about quantum computation (QC) and quantum information processing (QIP) has been restless growing. Applications of QIP e.g., quantum cryptography and quantum teleportation, have been proposed and verified experimentally. In QC it has been shown that quantum algorithms may speed up some classically intractable problems in computer science [1].

Unfortunately this power inherent to quantum features (i.e., entanglement, state superposition) is difficult to be exploited because quantum states are typically highly unstable: the undesired coupling with the many degrees of freedom of the environment may lead to decoherence and to loss of the information encoded. Another source of error can be the imperfect control of parameters driving the evolution of the system. This can lead to wrong output states. To implement effective QIP techniques these two problems must be faced and solved.

For the problem of decoherence, some methods have been proposed theoretically: via error correcting codes [2] it is possible to find errors induced by the environment and correct them. Other approaches propose to encode information in states that are stable against environmental noise [3] or to eliminate dynamically the noise effects ([4],[5]). A few quantum hardwares have been proposed for implementation of quantum gates; e.g.: nuclear magnetic resonance [6], ion traps ([7], [8], [9], [10]) semiconductor quantum dots (or macroatoms) [11], [13]; in each of these implementations we have different gates and different ways of processing information.

A conceptually novel approach is *topological computation* [14],[15] in which the gate parameters depends only on global features of the control process, being therefore insensitive to local fluctuations. Though interesting the topological gates proposed so far are quite difficult to realize in practice because they are based on of non-local quantum states of many body systems with complicate interactions.

Another approach that keeps some of the global (geometrical) features of the quantum gates and seems closer

to today experimental technology, is the the so-called *Holonomic Quantum Computation* (HQC) ([16], [17]). In this paper we shall analyze in a detailed manner a recent proposal for HQC with semiconductor quantum dots [18].

We shall start by recalling the basic facts about HQC (Sect. II) and on excitonic transitions in semiconductor macroatoms (Sect. III) In Sect IV we will show how to encode quantum information in excitonic state an how to realize single-qubit gates by means of laser pulses. Two-qubit gates resorting to bi-excitonic shift are illustrated in Sect V. Sect. VI contains the conclusions and an appendix is added to improve the self-consistency of the paper.

## II. QUANTUM HOLONOMIES

When a quantum state undergoes an adiabatic cyclic evolution, a nontrivial phase factor appears. This is called *geometrical phase* because it only depends on global properties, i.e, not on the path in the parameter space but only on the swept solid angle. If the evolving state is non-degenerate we have only an Abelian phase (Berry phase [19]), but if it is degenerate we have a non-Abelian operator. Then we can use it to process the quantum information encoded in the state.

More precisely, if we have a family  $\mathcal{F}$  of isodegenerate Hamiltonians  $H(\lambda)$  depending on  $m$  dynamically controllable parameters  $\lambda$ , we encode the information in a  $n$ -fold degenerate eigenspace  $\mathcal{E}$  of an Hamiltonian  $H(\lambda_0)$ . Changing the  $\lambda$ 's and driving  $H(\lambda)$  along a loop we produce a non-trivial transformation of the initial state  $|\psi_0\rangle \rightarrow U|\psi_0\rangle$ .

These transformations, called *holonomies*, are the generalization of Berry's phase and can be computed in terms of the Wilczek-Zee gauge connection [20]:  $U(C) = \mathbf{P} \exp(\oint_C A)$  where  $C$  is the loop in the parameter space and  $A = \sum_{\mu=1}^m A_{\mu} d\lambda_{\mu}$  is the  $u(n)$ -valued connection. If  $|D_i(\lambda)\rangle$  ( $i = 1, \dots, n$ ) are the instantaneous eigenstates of  $H(\lambda)$ , the connection is  $(A_{\mu})_{\alpha\beta} = \langle D_{\alpha} | \partial / \partial \lambda_{\mu} | D_{\beta} \rangle$  ( $\alpha,$

$\beta = 1, \dots, n$ ).

It is useful to introduce the *curvature* 2-form  $F = \sum_{\mu\nu} F_{\mu\nu} dx^\mu \wedge dx^\nu$  where  $F_{\mu\nu} = \partial_\mu A_\nu - \partial_\nu A_\mu + [A_\mu, A_\nu]$ ;  $F$  allow us to evaluate the dimension of the holonomy group and when this coincides with the dimension of  $U(n)$  we are able to perform universal quantum computation with holonomies.

For computation purposes we note that if the connection components commute  $[A_\mu, A_\nu] = 0$ , the curvature reduces to  $F_{\mu\nu} = \partial_\mu A_\nu - \partial_\nu A_\mu$  and we can use Stoke's theorem to compute the holonomies. The holonomic transformation can be calculated easier  $U = \exp(i \int_S F_{\mu\nu} d\lambda_\mu \wedge d\lambda_\nu)$  and depends on the 'flux' of  $F_{\mu\nu}$  through the surface  $S$  delimited by  $C$ . It is now clear that holonomies are associated to geometrical features of the parameter space.

Even if with an holonomy we can build every kind of transformation (logical gate) it is useful to think in terms of few simple gates that constitute an universal set (i.e., which can be composed to obtain any unitary operator).

Many efforts have been made to implement geometrical quantum gates (i.e. nuclear magnetic resonance [21] or super-conducting nanocircuits [22]) because they are believed to be fault tolerant for errors due to an imperfect control of parameters [23], [24]. Non-adiabatic realizations of Berry's phase logic gates have been studied as well [25], [26],[27]. More recently, schemes for the experimental implementation of non-Abelian holonomic gates have been proposed for atomic physics, [28] ion traps [29], Josephson junctions [30], Bose-Einstein condensates [31] and neutral atoms in cavity [32].

The basic idea is to have a four level  $\Lambda$  system with an excited state ( $|e\rangle$ ) connected to a triple degenerate space with the logical qubits ( $|0\rangle$  and  $|1\rangle$ ) and an *ancilla* qubit ( $|a\rangle$ ); the three degenerate state are separately addressed and controlled. The effective interaction Hamiltonian describing the system is (in interaction picture)

$$H_{int} = \hbar|e\rangle\langle 0| + \Omega_1|1\rangle + \Omega_a|a\rangle + h.c. \quad (1)$$

$H$  possesses a two degenerate states (called *dark states*) with  $E(t) = 0$  and two *bright states* with  $E(t) = \pm\Omega$  ( $\Omega = \sqrt{|\Omega_0|^2 + |\Omega_1|^2 + |\Omega_a|^2}$ ). At  $t = 0$  we codify the logical information in one of these *dark states* (i.e.,  $|0\rangle$  or  $|1\rangle$ ) and then, changing the Rabi frequencies ( $\Omega_i$ ,  $i = 0, 1, a$ ) we perform a loop in the parameter space ( $H(0) = H(T)$ ). If the adiabatic condition is full-filled at a generic time  $t$  the state of the system will be a *dark state* of  $H(t)$  and to the hamiltonian loop will correspond a loop for the state vector. Since for the adiabatic condition the excited state is never populated, the instantaneous *dark state* will be a superposition of the degenerate states. With this loop we produce a rotation in the degenerate space ( $|0\rangle$ ,  $|1\rangle$ ,  $|a\rangle$ ) starting from a logical qubit and passing through the *ancilla* qubit. At the beginning and at the end of the cycle we have only logical bits, but after a loop a geometrical operator is applied to them. Since we can

TABLE I:  $\Gamma_6$  (conduction band),  $\Gamma_7$ ,  $\Gamma_8$  periodic part of Bloch function.

$ J_{tot}, J_z\rangle$	$\Psi$	$\Gamma$
$ \frac{1}{2}, \frac{1}{2}\rangle$	$i S \uparrow\rangle$	$\Gamma_6$
$ \frac{1}{2}, -\frac{1}{2}\rangle$	$i S \downarrow\rangle$	$\Gamma_6$
$ \frac{3}{2}, \frac{3}{2}\rangle$	$\frac{1}{\sqrt{2}} (X + iY) \uparrow\rangle$	$\Gamma_8$ (HH)
$ \frac{3}{2}, -\frac{3}{2}\rangle$	$\frac{1}{\sqrt{2}} (X - iY) \downarrow\rangle$	$\Gamma_8$ (HH)
$ \frac{3}{2}, \frac{1}{2}\rangle$	$-\sqrt{\frac{2}{3}} Z \uparrow\rangle + \frac{1}{\sqrt{6}} (X + iY) \downarrow\rangle$	$\Gamma_8$ (LH)
$ \frac{3}{2}, -\frac{1}{2}\rangle$	$-\sqrt{\frac{2}{3}} Z \downarrow\rangle - \frac{1}{\sqrt{6}} (X - iY) \uparrow\rangle$	$\Gamma_8$ (LH)
$ \frac{1}{2}, \frac{1}{2}\rangle$	$\frac{1}{\sqrt{3}} Z \uparrow\rangle + \frac{1}{\sqrt{3}} (X + iY) \downarrow\rangle$	$\Gamma_7$
$ \frac{1}{2}, -\frac{1}{2}\rangle$	$\frac{1}{\sqrt{3}} Z \downarrow\rangle + \frac{1}{\sqrt{3}} (X - iY) \uparrow\rangle$	$\Gamma_7$

diagonalize (1) it is easy to calculate the connection and the holonomy associated to the loop.

We can construct two single qubit gates :  $U_1 = e^{i\phi_1|1\rangle\langle 1|}$  (*selective phase shift*) and  $U_2 = e^{i\phi_2\sigma_y}$  ( $\sigma_y = i(|1\rangle\langle 0| - |0\rangle\langle 1|)$ ). These two gates ( $U_1$  and  $U_2$ ) are non-commutable, so we can construct non-Abelian holonomies since  $U_1U_2 \neq U_2U_1$ .

To obtain an universal set of gates we must introduce a two bit gate; since these gates exploit the interaction between two qubits they will depend on the physical systems considered. A common choice ([29], [18]) is to realize a *selective phase shift* gate  $U_3 = e^{i\phi_3|11\rangle\langle 11|}$ .

### III. EXCITONIC TRANSITIONS

In what follows we show that if we can act on a quantum dot with coherent optical (laser) pulses, we can produce Coulomb-correlated electron-hole pairs (excitons) and we deal with an interaction Hamiltonian similar to the one described in (1). By changing the laser parameters along the adiabatic loop, we can produce the same single qubit gates as in [29].

In the GaAs-based III-V compounds the six electrons in the valence band are divided in a quadruplet ( $\Gamma_8$  symmetry) which corresponds to  $J_{tot} = 3/2$ , and a doublet ( $\Gamma_7$  symmetry) which corresponds to  $J_{tot} = 1/2$ . If we consider a GaAs/AlGaAs quantum dot, the confining potential (along the  $z$  growth axis) breaks the symmetry and lifts the degeneracy [33]. The states of the quadruplet are separated in  $J_z = \pm 3/2$  (*heavy holes*) and  $J_z = \pm 1/2$  (*light holes*). The  $\Gamma_7$  electrons have  $J_z = \pm 1/2$ . We can rewrite the eigenstates of  $J_{tot}$  and  $J_z$  using the  $|S\rangle$ ,  $|X\rangle$ ,  $|Y\rangle$ ,  $|Z\rangle$  states (the four  $\Gamma$  point Bloch function, table I).

If we shine the quantum dot with a laser beam we excite an electron from the valence band to the conduction band. In the dipole approximation we have to calculate the amplitude transition  $\langle f|\epsilon \cdot \mathbf{r}|i\rangle$  (where  $\epsilon$  is the polarization vector of the electromagnetic wave,  $|i\rangle$  and  $|f\rangle$  are the initial and final state respectively).

The only non-vanishing transition amplitudes for our calculations are  $\langle S|x|X\rangle$ ,  $\langle S|y|Y\rangle$ ,  $\langle S|z|Z\rangle$ .

Using this relation and table I we can calculate which transitions are allowed and which ones are forbidden.

First we note that, for states like  $|(X + iY)\rangle$ , we can have a transition only using 'negative' circular polarization light  $\epsilon = \epsilon_x - i\epsilon_y$ .

$$\begin{aligned} \langle S|\epsilon \cdot r|(X + iY)\rangle &= \langle S|(x - iy)|(X + iY)\rangle = \\ &= \langle S|x|X\rangle + \langle S|y|Y\rangle = 2\langle S|x|X\rangle \quad (2) \end{aligned}$$

( $\langle S|x|X\rangle = \langle S|y|Y\rangle$  for the symmetry of our system).

Using "positive" circularly polarized light we have no transition

$$\begin{aligned} \langle S|\epsilon \cdot r|(X + iY)\rangle &= \langle S|(x + iy)|(X + iY)\rangle = \\ &= \langle S|x|X\rangle - \langle S|y|Y\rangle = 0 \quad (3) \end{aligned}$$

The latter are called *polarizations selection rules (PSR)*.

We have also to consider the spin wave function in the initial and final state. If the initial state has spin up (down) the final state must have spin up (down) (*spin selection rules (SSR)*). For example:

$$\langle S|(x - iy)|(X + iY)\rangle \langle \uparrow | \uparrow \rangle = 2\langle S|x|X\rangle$$

$$\langle S|(x - iy)|(X + iY)\rangle \langle \uparrow | \downarrow \rangle = 0 \quad (4)$$

### A. Heavy-hole transitions

From table I we have the *heavy hole* and the  $\Gamma_6$  (conduction band) states; using *SSR* we can say that the only allowed transitions are

$$\begin{aligned} |\frac{3}{2}, \frac{3}{2}\rangle &= \frac{1}{\sqrt{2}}|(X + iY)\uparrow\rangle \rightarrow |\frac{1}{2}, \frac{1}{2}\rangle = i|S\uparrow\rangle \\ |\frac{3}{2}, -\frac{3}{2}\rangle &= \frac{1}{\sqrt{2}}|(X - iY)\downarrow\rangle \rightarrow |\frac{1}{2}, -\frac{1}{2}\rangle = i|S\downarrow\rangle \end{aligned}$$

The first transition is produced by "negative" circularly polarized light (we write the corresponding operator as  $\sigma^-$ ) and the second transition is produced by "positive" circularly polarized light ( $\sigma^+$ ) for the *PSR*.

In terms of excitons (electron-hole pairs) if we perform a transition with  $\sigma^-$ , we promote an electron with spin 3/2 of the valence band to the conduction band with spin 1/2 and we get an exciton with angular momentum  $-1$  ( $E^-$ ). With  $\sigma^+$  we promote an electron with spin  $-3/2$  of the valence band to the conduction band with spin 1/2 and we have an exciton with angular momentum 1 ( $E^+$ ).

### B. Light hole transitions

For the *light hole* we have more allowed transitions; this is due to the presence of the  $|Z\rangle$  states in the wave function. As for the HH transitions, using  $\sigma^\pm$  we have

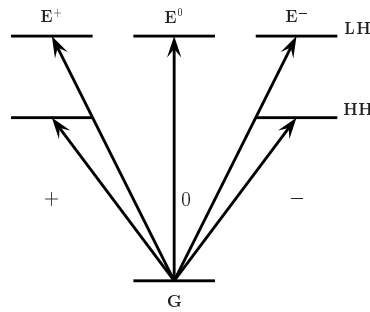


FIG. 1: Level scheme for LH and HH.

$$\begin{aligned} |\frac{3}{2}, \frac{1}{2}\rangle &\xrightarrow{\sigma^-} |\frac{1}{2}, -\frac{1}{2}\rangle \\ |\frac{3}{2}, -\frac{1}{2}\rangle &\xrightarrow{\sigma^+} |\frac{1}{2}, \frac{1}{2}\rangle \end{aligned}$$

These transitions are allowed with circular (positive or negative) polarization ( $\epsilon = \epsilon_x \pm i\epsilon_y$ ) and propagation along the  $z$  (growth) axis. If we have the wave propagating along the  $x$  or  $y$  axis and the polarization along  $z$  the transition is allowed by *PSR*. Using also the *SSR* we get the two allowed transitions:

$$\langle \frac{1}{2}, \frac{1}{2} | z | \frac{3}{2}, \frac{1}{2} \rangle \sim \langle S | z | Z \rangle \quad (5)$$

$$\langle \frac{1}{2}, -\frac{1}{2} | z | \frac{3}{2}, -\frac{1}{2} \rangle \sim \langle S | z | Z \rangle \quad (6)$$

With the operator  $\sigma^0$  we have the following transitions

$$\begin{aligned} |\frac{3}{2}, \frac{1}{2}\rangle &\xrightarrow{\sigma^0} |\frac{1}{2}, \frac{1}{2}\rangle \\ |\frac{3}{2}, -\frac{1}{2}\rangle &\xrightarrow{\sigma^0} |\frac{1}{2}, -\frac{1}{2}\rangle \end{aligned}$$

Such transitions with polarization along  $z$  have been experimentally observed [34].

Exciting light-hole electrons with three different kinds of light (left and right circular polarization and polarization along  $z$  axis) we can induce three different kinds of transitions with the same energy [34].

In terms of excitons if we make a transition with  $\sigma^\pm$ , we promote an electron with spin  $\mp 1/2$  from the valence band to the conduction band with spin  $\pm 1/2$  and we get an exciton with angular momentum  $\pm 1$  ( $E^\pm$ ). Using light propagating along  $x$  or  $y$  with  $z$  polarization we promote an electron with spin  $\pm 1/2$  from the valence band to the conduction band with spin  $\pm 1/2$  and we have an exciton with angular momentum 0 ( $E^0$ ).

The allowed transitions and the corresponding energy-level scheme for HH and LH are shown in fig. 1.

### C. $\Gamma_7$ transitions

In the same way we can compute the transition selection rules for the  $\Gamma_7$  electrons.

$$\begin{aligned}
|\frac{1}{2}, \frac{1}{2}\rangle & \xrightarrow{\sigma^-} |\frac{1}{2}, -\frac{1}{2}\rangle \\
|\frac{1}{2}, -\frac{1}{2}\rangle & \xrightarrow{\sigma^+} |\frac{1}{2}, \frac{1}{2}\rangle \\
|\frac{1}{2}, \frac{1}{2}\rangle & \xrightarrow{\sigma^0} |\frac{1}{2}, \frac{1}{2}\rangle \\
|\frac{1}{2}, -\frac{1}{2}\rangle & \xrightarrow{\sigma^0} |\frac{1}{2}, -\frac{1}{2}\rangle
\end{aligned}$$

Like for the LH, we have three different kinds of transitions that can be distinguished by the light polarization.

Those transitions are energetically higher with respect to the LH and HH ones. Therefore, we should be able to inhibit them using properly tuned laser sources with bandwidth  $\Delta E < E_{\Gamma_7} - E_{LH} \simeq 0.3 \text{ eV}$  [35].

#### IV. EXCITON INTERACTION HAMILTONIAN AND SINGLE QUBIT GATES

Now we want to write the interaction Hamiltonian for the exciton transitions (excluding  $\Gamma_7$  transitions).

The Hamiltonian for the light-matter interaction is (we use the electric field instead of the vector potential [36])

$$H_{int} = -e[\vec{P} \cdot \vec{E}^*(t) + h.c.] \quad (7)$$

where  $\vec{E}(t)$  is the electric field,  $\vec{P}$  is the polarization operator defined as

$$\vec{P} = \sum_{n,m} v_m^\dagger c_n \langle v, m | e\vec{r} | c, n \rangle = \sum_{n,m} v_m^\dagger c_n \vec{\mu}_{nm}^* \quad (8)$$

and

$$\vec{\mu}_{nm} = \langle c, n | e\vec{r} | v, m \rangle \quad (9)$$

$c_n$  and  $c_n^\dagger$  are the annihilation and creation operator for an electron in the conduction band with spin  $n$  ( $n = \pm 1/2$ );  $v_m$  and  $v_m^\dagger$  are the annihilation and creation operators for an electron in the valence band with spin  $m$  ( $m = \pm 1/2$  (LH) or  $m = \pm 3/2$  (HH)).

Then, using the dipole approximation ( $\vec{E}^*(t) = E_0 e^{i(\mathbf{k}\mathbf{x} - \omega t)} \epsilon \approx E_0 e^{-i\omega t} \epsilon$ )

$$H_{int} = -[\sum_{n,m} v_m^\dagger c_n \langle v, m | e\vec{r} | c, n \rangle \cdot \vec{E}^*(t) + h.c.] \quad (10)$$

We define

$$\hbar\Omega_{n,m} = \vec{\mu}_{nm}^* \cdot \vec{E}^*(t) = E_0 e^{-i\omega t} \epsilon \cdot \langle v, m | e\vec{r} | c, n \rangle \quad (11)$$

The last term is the dipole transition amplitude.

The term  $c_{\pm 1/2}^\dagger v_{\pm 3/2}$  describes the promotion of an electron with spin  $\pm 3/2$  to the conduction band with spin  $\pm 1/2$  and then it describes the creation of an 'heavy' exciton with angular momentum  $\pm 1$  ( $E^\pm$ ) from the ground

TABLE II: Rabi frequencies for allowed transitions.

$\Omega_{n,m}$	v		c	exciton
$\Omega_{\frac{1}{2}, \frac{3}{2}}$	$\frac{3}{2}$	$\rightarrow$	$\frac{1}{2}$	$E^-$
$\Omega_{-\frac{1}{2}, -\frac{3}{2}}$	$-\frac{3}{2}$	$\rightarrow$	$-\frac{1}{2}$	$E^+$
$\Omega_{\frac{1}{2}, -\frac{1}{2}}$	$-\frac{1}{2}$	$\rightarrow$	$\frac{1}{2}$	$E^+$
$\Omega_{-\frac{1}{2}, \frac{1}{2}}$	$\frac{1}{2}$	$\rightarrow$	$-\frac{1}{2}$	$E^-$
$\Omega_{\frac{1}{2}, \frac{1}{2}}$	$\frac{1}{2}$	$\rightarrow$	$\frac{1}{2}$	$E^0$
$\Omega_{-\frac{1}{2}, -\frac{1}{2}}$	$-\frac{1}{2}$	$\rightarrow$	$-\frac{1}{2}$	$E^0$

state ( $G$ ). In the same way we can rewrite the terms in (10) taking account of *light hole* transition. With this new notation, we have non-vanishing coefficients (as discussed in section III) in table II.

The Hamiltonian becomes

$$\begin{aligned}
H_{int} = & -\hbar[\Omega_{-,HH}|E_H^- \rangle \langle G| + \Omega_{+,HH}|E_H^+ \rangle \langle G| + \\
& \Omega_{+,LH}|E_L^+ \rangle \langle G| + \Omega_{-,LH}|E_L^- \rangle \langle G| + \\
& \Omega_{0,LH}|E_L^0 \rangle \langle G| + h.c.] \quad (12)
\end{aligned}$$

In the last term we include the two identical kinds of  $E^0$  excitons.

As we stated before, if we can address the light or heavy hole we can distinguish between  $E_{HH}^\pm$  and  $E_{LH}^\pm$ ; so using light with specified frequency tuned to LH transition, we can write:

$$\begin{aligned}
H_{int} = & -\hbar(\Omega_{+,LH}|E_L^+ \rangle + \Omega_{-,LH}|E_L^- \rangle + \Omega_{0,LH}|E_L^0 \rangle) \langle G| \\
& + h.c. \quad (13)
\end{aligned}$$

This Hamiltonian has the same structure as the one proposed in [29] to implement the holonomic quantum computation with trapped ions. So we can construct the same geometrical single qubit gates ( $U_1$  and  $U_2$ ) using, for example,  $E^+$  and  $E^-$  as  $|1\rangle$  and  $|0\rangle$  bits respectively and  $E^0$  as *ancilla* bit  $|a\rangle$ .

For the first gate we choose  $\Omega_- = 0$ ,  $\Omega_+ = -\Omega \sin(\theta/2) e^{i\varphi}$  and  $\Omega_0 = \Omega \cos(\theta/2)$ . The dark states are given by  $|E^-\rangle$  and  $|\psi\rangle = \cos(\theta/2)|E^+\rangle + \sin(\theta/2) e^{i\varphi}|E^0\rangle$ . By evaluating the connection associated to this two-dimensional degenerate eigenspace, it is not difficult to see that the unitary transformation  $U_1 = e^{i\phi_1|E^+\rangle\langle E^+|}$  ( $\phi_1 = \frac{1}{2} \oint \sin\theta d\theta d\varphi$ ) can be realized as an holonomy. For the second gate we choose  $\Omega_- = \Omega \sin\theta \cos\varphi$ ,  $\Omega_+ = \Omega \sin\theta \sin\varphi$  and  $\Omega_0 = \Omega \cos\theta$ . The dark states are now given by  $|\psi_1\rangle = \cos\theta \cos\varphi|E^-\rangle + \cos\theta \sin\varphi|E^+\rangle - \sin\theta|E^0\rangle$  and  $|\psi_2\rangle = \cos\varphi|E^+\rangle - \sin\varphi|E^-\rangle$ . In this case, the unitary transformation  $U_2 = e^{i\phi_2\sigma_y}$  (where  $\phi_2 = \oint \sin\theta d\theta d\varphi$  and  $i\sigma = |E^+\rangle\langle E^-| - |E^-\rangle\langle E^+|$ ) can be implemented.

We performed numerical simulations to show how our scheme works and how we can satisfy adiabaticity request and apply logical gates. The exciton states have energies

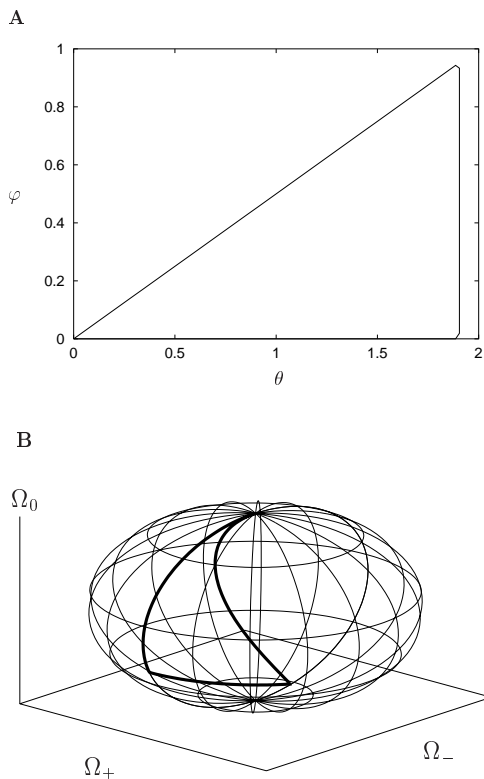


FIG. 2: (A) Loop in the  $\theta - \phi$  parameter space ( $\theta_m = \pi$ ). (B) Evolution of the  $|E^+\rangle$  in the  $|E^-\rangle - |E^+\rangle - |E^0\rangle$  space for gate 2 and  $\phi_2 = \pi/2$ .

between 1.5 eV and 1.7 eV which correspond to sub-femto second time scale; then using femtosecond laser pulse we avoid transition between *ground* and exciton state during the evolution. Using Rabi frequencies about  $0.02 \text{ fs}^{-1}$  (corresponding to  $\Omega^{-1} = 50 \text{ fs}$ ) and evolution times of  $T_{ad} = 7.5 \text{ ps}$  (as in the simulation) we get for the adiabatic condition  $\Omega T_{ad} = 150 \gg 1$  which assures us that there will be no transition between *dark* and *bright* states (separated by  $\Omega$  energy).

In Figure 2(A) the loop in the  $\theta - \phi$  space is shown. Since the holonomic operator depends on the solid angle ( $\oint d\Omega = \oint d\theta d\phi \sin \theta$ ), the only contribute from this loop comes from the first part and can be easily calculated  $\int d\Omega = 1/2(\sin \theta_m - \theta_m \cos \theta_m)$ . Then it is sufficient to change  $\theta_m$  to apply a different operator. In Fig. 2 (B) we show the loop in the control parameters manifold for gate 2 ( $\Omega^-, \Omega^+, \Omega^0$ ), since the parameters are real the 3D vector  $\vec{\Omega}$  evolves on a sphere. These two figures refer to the implementation of Hadamard gate (also shown in Fig. 3 (B) and in Fig. (4) ) and we choose  $\theta_m$  in order to obtain  $\oint d\Omega = \pi/4$ .

Figure 3 shows the state populations during the quantum-mechanical evolution; as we can see, the state  $|G\rangle$  is never populated (as expected in the adiabatic limit). For the case of gate 1 [see Fig. 3(A)] the  $|E^-\rangle$

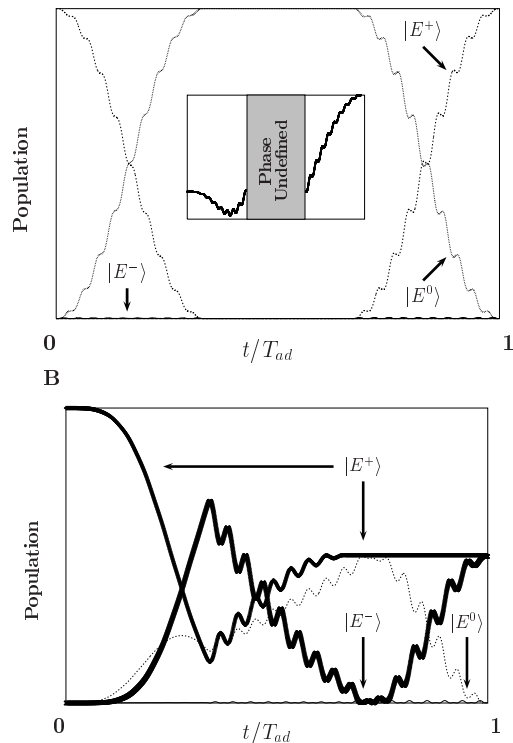


FIG. 3: (A) Simulated time evolution of the HQC gate 1 with  $\phi_1 = \pi/4$  and initial state  $|E^+\rangle$ . The inset shows (where it is defined) the quantity  $\varphi$  where  $\varphi := \text{Arg}\langle\Psi(t)|E^+\rangle/|\langle\Psi(t)|E^+\rangle|$ . (B) Simulated time evolution of the HQC gate 2 with  $\phi_2 = \pi/4$  (Hadamard gate) and initial state  $|E^+\rangle$ .

state is decoupled in the evolution while the state  $|E^+\rangle$  evolves to the *ancilla* state ( $|E^0\rangle$ ), to eventually end in  $|E^+\rangle$  (as we expect for the dark state). In the inset we show the phase accumulated by the  $|E^+\rangle$  state; of course, in the central region the phase is undefined.

The quantum evolution of gate 2 in Fig. 3(B) is more complicated because there are not decoupled states and all the three degenerate states are populated. We start from  $|E^+\rangle$  and end in a superposition of  $|E^+\rangle - |E^-\rangle$ . It can be better understood by looking at Fig. 4, where we show the evolution of the dark state in the  $|E^+\rangle, |E^-\rangle, |E^0\rangle$  space. As mentioned above, the initial dark state evolves in the degenerate space: it starts from the  $|E^+\rangle$  axis, then passes through a superposition of the three states and ends in the  $|E^+\rangle - |E^-\rangle$  plane ( $(|E^+\rangle + |E^-\rangle)/\sqrt{2}$  state).

The numerical simulations show that our scheme works and we are able to produce the desired gates with realistic parameters for the semiconductor quantum dots [37] and for the recent ultrafast laser technology [38]. Moreover it is clear (also with the gates in [18]) that we are able to apply different gates in the same gating time because the latter depends only on the adiabatic constraint (and not on the gate we choose) and though the adiabatic limitation we can apply several quantum gates. Infact recent

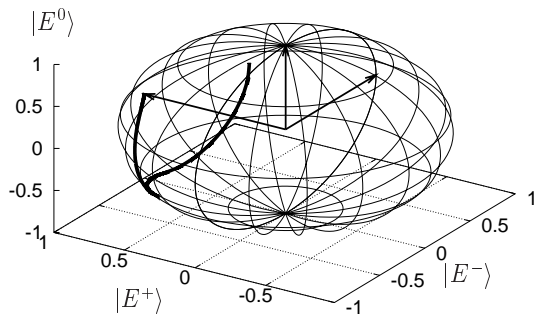


FIG. 4: Evolution of the initial state  $|E^+\rangle$  in the  $|E^-\rangle - |E^+\rangle - |E^0\rangle$  space for gate 2 and  $\phi_2 = \pi/2$ .

studies [39] have shown that excitons can exhibit a long dephasing time (comparable to hole-electron recombination time) on nanosecond time-scale. The degeneracy in our model has an important role (even if the request can be made weaker and we can use almost-degenerate state i.e. see section IV A) and this can further prolong the decoherence time till the recombination of light-hole.

### A. Laser bandwidth

We saw that by using light with different polarizations we can induce different transitions and generate  $E^\pm$ ,  $E^0$  excitons. To select which electron to excite (HH, LH,  $\Gamma_7$ ) we have to use different energies; in fact the  $\Gamma_7$  transitions are the most energetic, then there are the LH and the HH.

For circular ( $\pm$ ) polarization light propagating along the  $z$  axis we have [35] that the ratio of probabilities to excite the relative electron is

$$\frac{\text{HH}}{\text{LH}} = 3$$

$$\frac{\text{HH}}{\Gamma_7} = \frac{3}{2}$$

So it is sufficient that the laser bandwidth is not too large ( $\Delta E < E_{\text{LH}} - E_{\text{HH}}$  but  $\Delta E \ll E_{\Gamma_7} - E_{\text{LH}}$ ) to excite HH instead of LH and forbid the  $\Gamma_7$ .

For light propagating along the  $x(y)$  axis with  $z$  polarization the HH transition are forbidden and

$$\frac{\text{LH}}{\Gamma_7} = 2$$

So even if this laser bandwidth is  $\Delta E < E_{\Gamma_7} - E_{\text{LH}}$  it is more likely to produce LH. As we wrote before in practical situation we should be able to prohibit  $\Gamma_7$  transition just with this choices.

Now we show that even if we are not able to energetically distinguish HH and LH the holonomic scheme proposed works as usually. The level scheme for this configuration is shown in Fig 5. We can excite  $E_{\text{HH}}^\pm$  excitons or  $E_{\text{LH}}^0$  exciton. If we have an adiabatic evolution fast enough, the three levels are mixed during the evolution

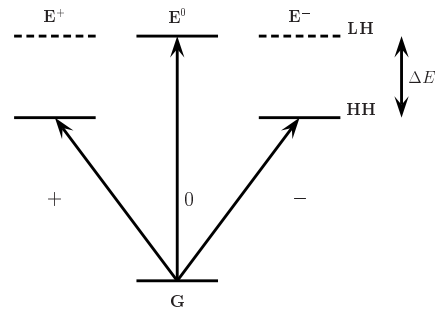


FIG. 5: Level scheme for geometrical gates when it is impossible to address only HH or LH.

and so, for our scheme, they can be considered degenerate.

The energy gap between HH and LH excitons is of the order of  $0.05 - 0.03 \text{ eV}$  ([34], [40], [41], [42]), whereas between  $\Gamma_7$  and HH-LH the gaps is about  $0.3 \text{ eV}$ . Both of this energy gap are very large compared to the bandwidth of the pico and femtosecond pulsed laser, so in practical applications one should be able to separate LH and HH excitons.

### B. Dynamical phase

During the evolution along the adiabatic loop the state acquire a dynamical phase in addition to the geometrical phase. In the first proposal of adiabatic gates with standard two level systems additional work is needed to eliminate this undesired phase. In ref. [43] they show how this dynamical phase can be eliminated: we have to run the geometrical gate several times in order to let the dynamical phases cancel each others. The drawback in this method is that we have to iterate several times the adiabatic gate and, because of the adiabatic condition, long time is needed to apply the final geometrical gate.

In this model, if we use LH excitons, the logical and the *ancilla* states are degenerate and the ground state is never populated during the evolution; so the dynamical phase shift is the same for the two logical qubits and can be neglected.

If we encode logical information in the HH excitons ( $\pm$ ) and use the LH exciton (0) as *ancilla* qubit we have an energy difference  $\Delta E$  and then a dynamical phase appears. Again, we can neglect it, because at the beginning (encoding of information) and at the end (reading information) of the evolution, the  $|E^0\rangle$  state is never populated and then the phase difference does not affect the logical information. Then, in both models, we can avoid problems with the dynamical phase.

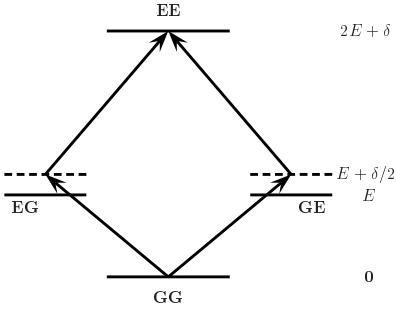


FIG. 6: Level scheme for the two-photon process.

## V. TWO QUBITS GATE

For the two qubit gate we cannot take directly the DCZ model but we use the bi-excitonic shift [13]. In fact if we have two coupled quantum dots the presence of an exciton in one of them (e.g. in dot b) produces a shift in the energy level of the other (e.g. dot a) from  $E$  to  $E + \delta/2$ .

Let's consider the two dots in the ground state  $|GG\rangle$ ; if we shine them with circular ('positive' or 'negative') light at  $E + \delta/2$  energy we should be able to produce two excitons  $|EE\rangle$  (see appendix A). For energy conservation this is the only possible transition (the absorption of a single photon is at energy  $E$ ). The detuning allows us to isolate the two-exciton space ( $|EE\rangle$ ) from the single exciton space ( $|EG\rangle, |GE\rangle$ ). The level scheme is shown in Fig. 6.

To show how the two-photon process happens we solved numerically the Schrodinger equation for a four-level system ( $|EE\rangle, |EG\rangle, |GE\rangle, |GG\rangle$ ). In Fig. 7 (A) we show the population evolution of the states; the Rabi oscillation between  $|EE\rangle$  and  $|GG\rangle$  are evident and the states  $|EG\rangle, |GE\rangle$  are never populated. In order to fulfill the perturbation condition we choose  $\delta/\Omega = 25$ .

We have another degree of freedom in our system: the polarization. Shining the dot with circular or linear polarization and we will obtain  $|GG\rangle \rightarrow |E^i E^j\rangle$  ( $i, j = +, -, 0$ ) and can reproduce the scheme with polarized excitons. The general Hamiltonian for the two-photon process is (in interaction representation)

$$H_{int} = -\frac{2\hbar^2}{\delta} \sum_{i,j=+,-,0} (\tilde{\Omega}_i \tilde{\Omega}_j e^{i(\phi_i + \phi_j)} |E^i E^j\rangle \langle GG| + h.c.) \quad (14)$$

The total two-exciton space has dimension nine but we can restrict to four dimension space turning off two laser with the same polarization (i.e.  $-$  or  $0$ ) and because of this situation the scheme is slightly different for the one proposed in the other papers. In ref. [18] we show how to construct a phase gate; turning on the  $+$  and  $0$  lasers and modulating them to simulate the evolution in gate 1 we were able to obtain the geometrical operator  $U_3 = \exp(i\phi |E^+\rangle \langle E^+| \otimes \mathbb{1})$ . We can decouple the logical states

with negative energy but we still need four laser (two with  $+$  polarization and two with  $0$  polarization) to produce a loop in the  $|E^+\rangle^{\otimes 2} - |E^0\rangle^{\otimes 2}$  space. The  $+$  and  $0$  lasers must be resonant with the two-exciton transition, but in this scheme we also produce not-logical states  $|E^+ E^0\rangle$  and  $|E^0 E^+\rangle$  since have the same energy ( $\omega_i^+ + \omega_j^0 = 2E + \delta$ ). Then we have a bigger dark space with dimension three and the scheme is not directly repeated. A detailed calculation of the dark states is given in appendix B.

Now we show how to construct another two-qubit geometrical operator with the same scheme. Since in general an adiabatic loop will produce a superposition of *all* the dark states, we change laser polarization ( $0 \rightarrow -$ ) in order that the system can evolves in the logical space. We note that the space is big enough to produce non-trivial transformation even without the *ancilla* qubits.

We choose the single laser Rabi frequencies in order to have  $\Omega^{++} = \Omega \sin \frac{\theta}{2}$ ,  $\Omega^{--} = \Omega \cos \frac{\theta}{2}$ ,  $\Omega^{+-} = \Omega \sqrt{|\sin \frac{\theta}{2} \cos \frac{\theta}{2}|}$  and  $0 \leq \theta \leq 4\pi$ . The dark state are

$$\begin{aligned} |D_1\rangle &= \cos \frac{\theta}{2} |++\rangle - \sin \frac{\theta}{2} |--\rangle \\ |D_2\rangle &= \frac{1}{\sqrt{2}} (|+-\rangle - |-+\rangle) \\ |D_3\rangle &= \sqrt{\frac{|\sin \theta|}{1 + |\sin \theta|}} (\sin \frac{\theta}{2} |++\rangle + \cos \frac{\theta}{2} |--\rangle) \\ &\quad - \frac{1}{\sqrt{2(1 + |\sin \theta|)}} (|+-\rangle + |-+\rangle) \end{aligned} \quad (15)$$

The associated connection is

$$A_\theta = \begin{pmatrix} 0 & 1/2 \sqrt{\frac{|\sin \theta|}{1 + |\sin \theta|}} \\ -1/2 \sqrt{\frac{|\sin \theta|}{1 + |\sin \theta|}} & 0 \end{pmatrix} \quad (16)$$

Of course, for different values of  $\theta$ ,  $[A_\theta, A_{\theta'}] = 0$  and we can calculate the loop integral and then the holonomy. From numerical calculation we have  $\alpha = \oint 1/2 \sqrt{\frac{|\sin \theta|}{1 + |\sin \theta|}} d\theta = \int_0^{4\pi} 1/2 \sqrt{\frac{|\sin \theta|}{1 + |\sin \theta|}} d\theta = 3.6806$  we have for the holonomic operator

$$U = e^{-\alpha \sigma_x} = \begin{pmatrix} \cos \alpha & -\sin \alpha \\ \sin \alpha & \cos \alpha \end{pmatrix} \quad (17)$$

We write explicitly the final state using  $|D_1(4\pi)\rangle = |E^+\rangle^{\otimes 2}$  and  $|D_2(4\pi)\rangle = 1/\sqrt{2}(|E^+ E^-\rangle + |E^- E^+\rangle)$

$$\begin{aligned} U |E^+\rangle^{\otimes 2} &= \cos \alpha |E^+\rangle^{\otimes 2} \\ &\quad - \frac{\sin \alpha}{\sqrt{2}} (|E^+ E^-\rangle + |E^- E^+\rangle) \end{aligned} \quad (18)$$

This is an entangling gate, and then we have another non-trivial gate. In Fig. 7 we show the numerical simulation obtained solving the Schrodinger equation. It is

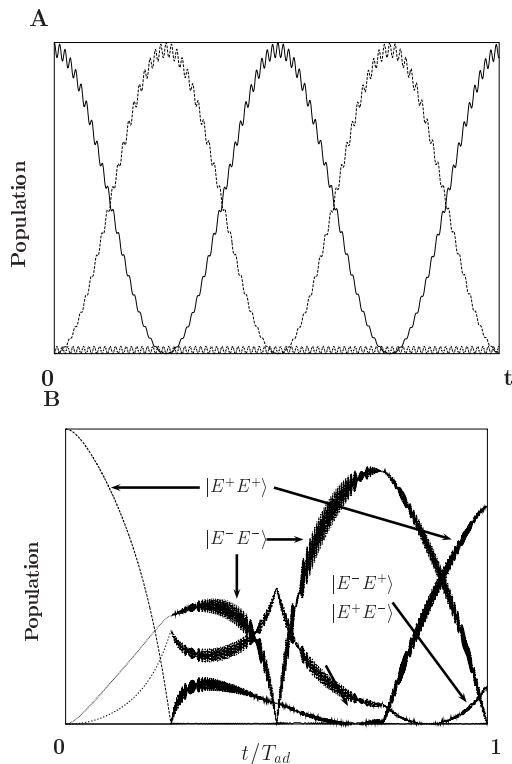


FIG. 7: (A) Production of a bi-exciton state and isolation of the  $|E^i\rangle^{\otimes 2} - |G\rangle^{\otimes 2}$  space with the detuned lasers. (B) Simulated population evolution for the two qubit phase gate.

difficult to follow the evolution of the states because of the number of the states populated during the evolution and because of the mixing of them. Moreover it can be

noted that the  $|GG\rangle$  state never appears in the evolution, the  $|E^-\rangle^{\otimes 2}$  state is not present at the end of the evolution and the final state is a superposition of  $|E^+\rangle^{\otimes 2}$  and (symmetrically)  $|E^+E^-\rangle - |E^-E^+\rangle$ .

## VI. CONCLUSIONS

In summary, we have shown that geometrical gates can be implemented in quantum dots with optical control. We use polarized excitons to encode logical information and we have been able to construct a universal set of geometrical quantum gates. The biexcitonic shift due to exciton-exciton dipole coupling is exploited to implement two qubit gates. Numerical simulations clearly suggest that one should be able to apply several holonomic gates within the decoherence time.

Even though the fault-tolerance features of this geometrical approach has not been completely clarified so far (see e.g., [44]), HQC surely provides, on the one hand, a sort of an intermediate step towards topological quantum computing and on the other hand, it is a natural arena in which to explore fascinating quantum phenomena.

Finally we hope that the theoretical investigations here presented will be effective in stimulating novel experimental activity in the field of coherent phenomena in semiconductor nanostructures.

## Acknowledgments

Funding by European Union project TOPQIP Project, (Contract IST-2001-39215) is gratefully acknowledged

- 
- [1] P.W. Shor *Proceeding of 35th Annual symposium on foundation of Computer Science*. (IEEE Computer Society Press, Los Alamitos, CA, 1994).
- [2] E. Knill, R. Laflamme, *Phys. Rev. A* **55**, 900 (1997) and references therein.
- [3] P. Zanardi and M. Rasetti, *Phys. Rev. Lett.* **79**, 3306 (1997).
- [4] L. Viola, E. Knill and S. Lloyd, *Phys. Rev. Lett.* **82**, 2417 (1999) and references therein.
- [5] P. Zanardi, *Phys. Lett. A* **258**, 77 (1999).
- [6] I.L. Chuang *et al.*, *Phys. Rev. Lett.* **80**, 3408 (1998).
- [7] J.I. Cirac and P. Zoller, *Phys. Rev. Lett.* **74**, 4091 (1995).
- [8] A. Sorensen and K. Molmer, *Phys. Rev. Lett.* **82**, 1971 (1999).
- [9] K. Molmer and A. Sorensen, *Phys. Rev. Lett.* **82**, 1935 (1999).
- [10] J.I. Cirac and P. Zoller, *Nature* **404**, 579 (2000)
- [11] D.P. DiVincenzo and D. Loss, *Phys. Rev. A* **57**, 120 (1998).
- [12] P. Zanardi and F. Rossi, *Phys. Rev. Lett.* **81**, 4752 (1998).
- [13] E. Biolatti *et al.*, *Phys. Rev. Lett* **85**, 5647 (2000).
- [14] A. Kitaev, Preprint quant-ph/9707021.
- [15] M.H. Freedman, A. Kitaev, W. Zhenghan, *Commun. Math. Phys.* **227** 587 (2002).
- [16] P. Zanardi and M. Rasetti, *Phys. Lett. A* **264**, 94 (1999).
- [17] J. Pachos, P. Zanardi and M. Rasetti, *Phys. Rev. A* **61**, 010305(R) (2000).
- [18] Solinas *et al.* quant-ph/0207019.
- [19] M.V. Berry, *Proc. R. Soc. Lond. A* **392**, 45 (1984).
- [20] F. Wilczek, A. Zee, *Phys. Rev. Lett.* **52**, 2111 (1984).
- [21] J.A. Jones *et al.*, *Nature* **403**, 869 (2000).
- [22] G. Falci *et al.*, *Nature* **407**, 355 (2000).
- [23] J. Preskill in *Introduction to Quantum Computation and Information*, edited by H.-K. Lo, S. Popescu, and T. Spiller (World Scientific, Singapore, 1999).
- [24] D. Ellinas and J. Pachos, *Phys. Rev. A* **64**, 022310 (2001).
- [25] W. Xiang-Bin and M. Keiji, *Phys. Rev. Lett.* **87**, 097901 (2001).
- [26] X.-Q. Li *et al.* Preprint (available at <http://arXiv.org/abs/quant-ph/0204028>).
- [27] P. Solinas *et al.* to be published.
- [28] R.G. Unanyan, B.W. Shore and K. Bergmann, *Phys. Rev. A* **59**, 2910 (1999).
- [29] L.-M. Duan, J. I. Cirac and P. Zoller, *Science* **292**, 1695 (2001).
- [30] L. Faoro, J. Siewert and R. Fazio, Preprint (available at

<http://arXiv.org/abs/cond-mat/0202217>;

- [31] I. Fuentes-Guridi *et al.* Phys. Rev. A **66**, 022102 (2002)  
 [32] A. Recati *et al.* Phys. Rev. A **66**, 032309 (2002)  
 [33] R.T. Collins *et al.*, Phys. Rev. B **36**, 1531 (1987).  
 [34] J.-Y. Marzin *et al.* , Phys. Rev. B **31**, 8298 (1985).  
 [35] G.Bastard , *Wave mechanics applied to semiconductor heterostructures* (les editions de physique).  
 [36] S.S. Schimtt-Rink *et al.* , Phys. Rev. B **46**, 10460 (1992).  
 [37] Bayer, M. *et al.* Science **291**, 451 (2001)  
 [38] J. Shah, *Ultrafast Spectroscopy of Semiconductors and Semiconductor Nanostructures* (Springer, Berlin, 1996).  
 [39] P. Borri, *et al.* Phys. Rev. Lett. **87**, 157401 (2001).  
 [40] R.C. Miller *et al.* , Phys. Rev. B **22**, 863 (1980).  
 [41] R.C. Miller *et al.* , Phys. Rev. B **24**, 1134 (1981).  
 [42] Y.Matsumoto *et al.* , Phys. Rev. B **32**, 4275 (1985).  
 [43] A. Ekert *et al.* J. Mod. Opt. **47(14-15)**, 2501, (2000).  
 [44] A. Nazir, T. P. Spiller, and W. J. Munro Phys. Rev. A **65**, 042303 (2002); A. Blais, A.-M.S. Tremblay, quant-ph/0105006

## APPENDIX A: TWO-PHOTON PROCESS

Here we show how two-photon process may occur in our system. Let's consider two coupled quantum dots. The energy level spacing in this case is different, in fact the presence of an exciton in one of them (e.g. in dot b) produces a shift in the energy level of the other (e.g. dot a) from  $E$  to  $E + \delta/2$ . We have the following Hamiltonian

$$H_0 = (2E + \delta)(|E\rangle\langle E|)^{\otimes 2} + E(|EG\rangle\langle EG| + |GE\rangle\langle GE|) \quad (\text{A1})$$

Using two lasers with frequencies  $\omega = (E + \delta/2)$  ( $\hbar = 1$ ) the interaction Hamiltonian is (we explicitly take into account the time dependence  $\Omega_i = \tilde{\Omega}_i e^{-i\omega t}$  from (11))

$$H_{int} = -\hbar \sum_{i=1,2} (\tilde{\Omega}_i e^{-i\omega t} |E_i\rangle\langle G_i| + \tilde{\Omega}_i^* e^{i\omega t} |G_i\rangle\langle E_i|) \quad (\text{A2})$$

The effective Hamiltonian for the process is (the apex 2 indicate that is a second order process)

$$H_{int}^{(2)} = -\hbar \tilde{\Omega} e^{-i\tilde{\omega} t} |E\rangle\langle G|^{\otimes 2} + h.c. \quad (\text{A3})$$

where  $\tilde{\omega} = 2\omega$  is the frequency that produces the transition between  $|GG\rangle$  and  $|EE\rangle$ . There are four possible states ( $|GG\rangle, |EG\rangle, |GE\rangle, |EE\rangle$ ); let the initial state be  $|GG\rangle$  and we want to know the amplitude coefficient for the  $|GG\rangle \rightarrow |EE\rangle$  (Fig. 6). To do this we use the interaction picture

$$\langle i | e^{iH_0 t/\hbar} H_{int} e^{-iH_0 t/\hbar} | j \rangle = \delta^{i(\omega_i - \omega_j)t} e^{\pm i\omega t} \langle i | \tilde{H}_{int} | j \rangle \quad (\text{A4})$$

(the matrix element  $\langle i | \tilde{H}_{int} | j \rangle$  is time independent) with the initial conditions  $|\psi(0)\rangle = |GG\rangle$  ( $|\psi(t)\rangle =$

$\sum c_{ij}(t) |ij\rangle$ ,  $i, j = E, G$ ),  $\omega' = \omega_{EE} - \omega_m$  and  $\omega'' = \omega_m$ , with perturbation theory to the second order we get ( $|m\rangle$ 's are the intermediate states  $|EG\rangle$  and  $|GE\rangle$  with energy  $E = \hbar\omega_m$ )

$$c_{EE}^{(2)}(t) = \left(-\frac{i}{\hbar}\right)^2 \sum_m \int_0^t d\tau_1 \langle EE | \tilde{H}_{int} | m \rangle e^{i(\omega' - \omega)\tau_1} \int_0^{\tau_1} d\tau_2 \langle m | \tilde{H}_{int} | GG \rangle e^{i(\omega'' - \omega)\tau_2} \quad (\text{A5})$$

Using  $\omega'' + \omega' - 2\omega = 0$ , performing the double integration we get

$$c_{EE}^{(2)}(t) = \left(-\frac{i}{\hbar}\right)^2 \sum_m \langle EE | \tilde{H}_{int} | m \rangle \langle m | \tilde{H}_{int} | GG \rangle \frac{1}{i(\omega'' - \omega)} \left(t - \frac{e^{i(\omega' - \omega)t} - 1}{i(\omega' - \omega)}\right) \quad (\text{A6})$$

The term  $1 - e^{i(\omega' - \omega)t} i(\omega' - \omega)$  oscillates, so the leading term is proportional to  $t$

$$c_{EE}^{(2)}(t) \approx \frac{i}{\hbar^2} \sum_m \frac{\langle EE | \tilde{H}_{int} | m \rangle \langle m | \tilde{H}_{int} | GG \rangle}{\omega'' - \omega} t \quad (\text{A7})$$

Now we go back to the second order Hamiltonian (A3) (two-photon process) and calculate the evolution ( $\Delta\omega = \omega_{EE} = 2\omega$  and  $\Delta\omega - \tilde{\omega} = 0$ )

$$c_{EE}^{(2)} = -\frac{i}{\hbar} \int_0^t dt_1 \langle EE | \tilde{H}_{int}^{(2)} | GG \rangle e^{i(\Delta\omega - \tilde{\omega})t_1} = -\frac{i}{\hbar} \langle EE | \tilde{H}_{int}^{(2)} | GG \rangle \int_0^t dt_1 = -\frac{i}{\hbar} (-\hbar \tilde{\Omega}) t = i \tilde{\Omega} t \quad (\text{A8})$$

The two  $c_{EE}^{(2)}$ 's are calculated to the same order, so using (A6) and (A8)

$$\tilde{\Omega} = \frac{1}{\hbar^2} \sum_m \frac{\langle EE | \tilde{H}_{int} | m \rangle \langle m | \tilde{H}_{int} | GG \rangle}{\omega'' - \omega} \quad (\text{A9})$$

In our system

$$\begin{aligned} & \langle EE | \tilde{H}_{int} | EG \rangle \langle EG | \tilde{H}_{int} | GG \rangle = \\ & = \langle EE | \tilde{H}_{int} | GE \rangle \langle GE | \tilde{H}_{int} | GG \rangle = \\ & = \hbar^2 \tilde{\Omega}_1 \tilde{\Omega}_2 \end{aligned} \quad (\text{A10})$$

and we have the Rabi frequency for the two-photon process as function of the single photon process ( $\omega_m'' - \omega = \delta/\hbar$ ).

$$\tilde{\Omega} = \frac{2\hbar \tilde{\Omega}_1 \tilde{\Omega}_2}{\delta} \quad (\text{A11})$$

We take into account the two exciton production for  $E^+$  and  $E^0$ , and choose:  $\tilde{\Omega}_{1i} = \tilde{\Omega}_i$ ,  $\tilde{\Omega}_{2i} = \Omega_i e^{i\varphi_i}$  with  $i = +, 0$ . The phenomenological Hamiltonian (A3) became

$$H_{int} = -\frac{2\hbar^2}{\delta} \tilde{\Omega}^2 e^{i\varphi} |E\rangle \langle G|^{\otimes 2} + h.c. \quad (\text{A12})$$

## APPENDIX B: HOLONOMIC STRUCTURE OF THE TWO-PHOTON PROCESS

To explicitly calculate the dark state of Hamiltonian (14) we change notation and include the phase in the definition of Rabi frequencies  $\Omega^{ij} = \tilde{\Omega}_i \tilde{\Omega}_j e^{i(\phi_i + \phi_j)}$ , rewrite the Hamiltonian taking account of production of the same spin excitons ( $i = j$ ) and choose the loop in order to have symmetric Rabi frequencies  $\Omega^{ij} = \Omega^{ji}$ , we obtain (with  $|E^i\rangle = |i\rangle$ ):

$$H_{int} = -\frac{2\hbar^2}{\delta} ((\Omega^{++})^* |++\rangle + (\Omega^{jj})^* |jj\rangle + (\Omega^{+j})^* (|+j\rangle + |j+\rangle)) \langle GG| + h.c. \quad (\text{B1})$$

where we can take  $j = 0, -$  to implement to different gates since we reduce the dark space and work with just two polarized excitons.

In addition to the decoupled states which do not appear in B1,

we have three dark states ( $\Omega^2 = |\Omega^{++}|^2 + |\Omega^{jj}|^2$ )

$$\begin{aligned} |D_1\rangle &= \frac{(\Omega^{jj})^* |++\rangle - (\Omega^{++})^* |jj\rangle}{\Omega} \\ |D_2\rangle &= \frac{1}{\sqrt{2}} (|+j\rangle - |j+\rangle) \\ |D_3\rangle &= \frac{1}{\Omega \sqrt{|\Omega^{ij}|^2 + \Omega^2/2}} [(\Omega^{ij})^* (\Omega^{++} |++\rangle + \Omega^{jj} |jj\rangle) \\ &\quad - \frac{\Omega^2}{2} (|+j\rangle + |j+\rangle)] \end{aligned} \quad (\text{B2})$$

Now we can explicitly calculate some connection for particular loops. we choose  $j = 0$  and for the laser

Rabi frequencies  $\Omega_i^+ = \sqrt{\Omega \sin(\theta/2)} \exp(i\varphi/2)$ ,  $\Omega_i^0 = \sqrt{\Omega \cos(\theta/2)}$  ( $i = 1, 2$  is the dot index) and we use a loop in the  $\theta$  and  $\phi$  plane similar to the one in figure 2 ( $0 \leq \theta \leq \pi$  and  $0 \leq \phi \leq \pi/2$ ); then we have for the effective Rabi frequencies

$$\begin{aligned} \Omega^{++} &= \Omega \sin \frac{\theta}{2} e^{i\varphi} \\ \Omega^{00} &= \Omega \cos \frac{\theta}{2} \\ \Omega^{+0} &= \Omega \sqrt{\sin \frac{\theta}{2} \cos \frac{\theta}{2}} \exp(i\varphi/2) \end{aligned} \quad (\text{B3})$$

The dark states in B2 explicitly take the form

$$\begin{aligned} |D_1\rangle &= \cos \frac{\theta}{2} |++\rangle - \sin \frac{\theta}{2} e^{-i\varphi} |00\rangle \\ |D_2\rangle &= \frac{1}{\sqrt{2}} (|+0\rangle - |0+\rangle) \\ |D_3\rangle &= \sqrt{\frac{\sin \theta}{1 + \sin \theta}} (\sin \frac{\theta}{2} e^{i\varphi/2} |++\rangle + \cos \frac{\theta}{2} e^{-i\varphi/2} |00\rangle) \\ &\quad - \frac{1}{\sqrt{2(1 + \sin \theta)}} (|+0\rangle + |0+\rangle) \end{aligned} \quad (\text{B4})$$

The connection associated is

$$A_\theta = \begin{pmatrix} 0 & 1/2 \sqrt{\frac{\sin \theta}{2 + \sin \theta}} e^{i\varphi/2} \\ -1/2 \sqrt{\frac{\sin \theta}{1 + \sin \theta}} e^{-i\varphi/2} & 0 \end{pmatrix} \quad (\text{B5})$$

$$A_\varphi = \begin{pmatrix} -i \sin^2 \frac{\theta}{2} & i/2 \sqrt{\frac{\sin \theta}{2 + \sin \theta}} \sin \theta e^{i\varphi/2} \\ i/2 \sqrt{\frac{\sin \theta}{1 + \sin \theta}} \sin \theta e^{-i\varphi/2} & i/2 \frac{\sin \theta}{1 + \sin \theta} \end{pmatrix} \quad (\text{B6})$$

The holonomic operator cannot be analytically calculated because the connections do not commute. Then we calculated it with computer simulations by discretization of the loop in the parameter space.